Simulation of microsegregation and microstructural evolution in directionally solidified superalloys

B. Böttger, U. Grafe, D. Ma, and S. G. Fries

A two-dimensional model for solidification and secondary phase precipitation in directionally solidified superalloys is presented, which makes use of a shape function approximation for the isothermal cross-section of the primary dendrites. The phase boundary is represented by a diffuse interface on a finite difference grid, as in phasefield methods. Thus, two-dimensional multicomponent diffusion can be calculated for all phases. Via a Fortran interface, the model is coupled to thermodynamic databases assessed using the 'calculation of phase diagrams' (Calphad) approach. In this way, for each time step actual data are available for partitioning, dendritic growth, and nucleation of secondary phases. The model is applied to Ni–Al–Cr as a ternary model system and to the commercial superalloy IN706. **MST/4802**

The authors are with ACCESS eV, Intzestrasse 5, D–52056 Aachen, Germany. Contribution to the 'Structure of materials' section of Materials Congress 2000 organised by IoM at Cirencester on 12–14 April 2000.
© 2000 IoM Communications Ltd.

Introduction

Solidification of multicomponent alloys such as nickel base superalloys under production conditions is always associated with solute redistribution of the alloying elements. Therefore, the formation of chemical inhomogeneities and the consequent precipitation of interdendritic phases may be observed. Such inhomogeneous microstructures may result in poor mechanical properties, even after heat treatment. For this reason it is important to predict segregation and secondary phase precipitation for different process parameters as well as for different alloy compositions.

In processes such as electroslag remelting (ESR) or vacuum arc remelting (VAR), dendritic growth in nickel base superalloys is normally near to the cellular–dendritic transition region because of the high thermal gradients. No tertiary arms are observed and the dendrites form a more or less regular array. For such cases one dimensional (1D) cylindrical models have been formulated, which use the primary dendritic distance λ_1 as the dimension of the unit cell.[1,2] Recently Ma[3] proposed a pseudo-2D model for cellular dendritic solidification of nickel base superalloys. This approach uses a fourfold shape function to describe the isothermal cross-section perpendicular to the growth direction of the dendrite.

Superalloys are complex multicomponent systems. Generally, the correct thermodynamic description is much more important than sophisticated kinetic modelling to obtain results that are comparable to experimental findings.[4] Multicomponent systems are often described by linearised or interpolated phase diagrams.[5,6] This is only a crude approximation, especially because tielines are not specified. Thermodynamic databases instead provide Gibbs energy phase descriptions of the system, based on a large number of experiments and assessed by the 'calculation of phase diagrams' (Calphad) approach.[7] By total Gibbs energy minimisation, phase equilibria can be obtained using software packages such as ThermoCalc.[8] In the case of superalloys, such databases have been developed to include up to 13 elements and also a large number of phases of practical interest.[9]

Unit cell approach

The model used in the present work is based on a unit cell approach for directional dendritic solidification, making use of a fourfold shape function for approximation of the isothermal cross-section of a dendrite such as that shown in Fig. 1, and was proposed by Ma[3]

$$L(\beta) = L_0(t)(1 + A\ \cos\ 4\beta) \quad . \quad . \quad . \quad . \quad . \quad . \quad . \quad . \quad (1)$$

The amplitude factor A determines the amount of anisotropy of the shape function. For $A = 0$ a circular shape is observed corresponding to cellular growth, and the maximum value is $A = 1$. The unit cell is depicted in Fig. 2 which also provides definitions of $L(\beta)$, L_0, and β; t is time.

The function is chosen according to the description of the surface free energy of fcc crystals.[10] Under the conditions of high thermal gradients and low cooling rates, no tertiary arms are observed and the shape function is a good geometric approach.

The side length of the unit cell is correlated to the dendritic primary spacing λ_1 and can be estimated from the thermal gradient G and the solidification velocity v using the theory of Hunt[11]

$$\lambda_1 = KG^{-1/2}v^{-1/4} \quad . \quad . \quad . \quad . \quad . \quad . \quad . \quad . \quad . \quad . \quad . \quad (2)$$

According to Goldschmidt[12] the factor K can be considered as a unique constant for superalloys. Alternatively, K can be estimated from experiments.

Shape constrained phasefield model

For numerical treatment of diffusion and dendritic growth, the shape function given by equation (1) is projected onto a finite differences grid. As in phasefield methods,[13,14] a diffuse interface is applied to avoid the necessity of front tracking and allow the application of a single diffusion algorithm to the entire multiphase region. The phasefield parameters ϕ_α are defined, which denote the local phase fractions of all phases α. The diffuse interface region is created by application of a hyperbolic tangent function perpendicular to the interface. The use of isolating boundary

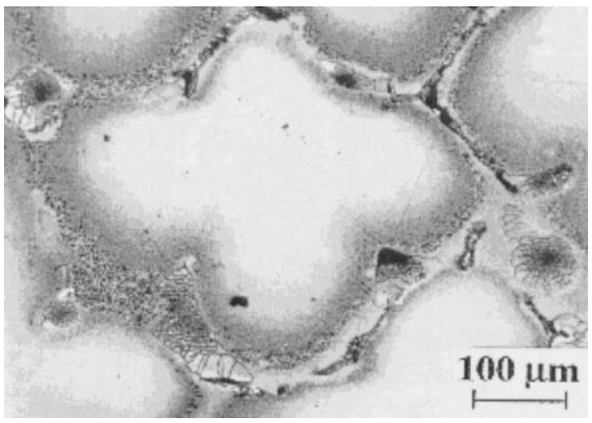

1 Isothermal cross-section through dendritic array [12] obtained by directional solidification

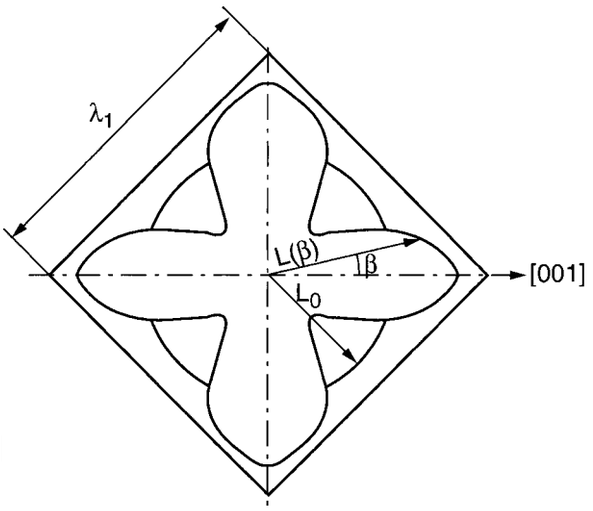

2 Dendritic unit cell for model

conditions at the border of the unit cell ensures proper treatment of the interaction with neighbouring dendrites for a regular dendritic array. For reasons of symmetry, only a quarter of the unit cell needs to be calculated.

MULTICOMPONENT DIFFUSION

The diffusion algorithm used in the shape constrained phasefield (SCPF) model is based on the multiphasefield diffusion concept[14] and has been generalised for multicomponent systems. The total flux of component k, i.e. $\mathrm{d}c^{\mathrm{k}}/\mathrm{d}t$ in the multiphase region is considered as the sum of the fluxes in the individual phases weighted by their phasefield parameter ϕ_α, which corresponds to the local volume fraction of phase α (volume average approach)

$$\mathrm{d}c^{\mathrm{k}}/\mathrm{d}t = \nabla \sum_{\alpha=1}^{\mathrm{N}} \phi_\alpha D_\alpha^{\mathrm{k}} \nabla c_\alpha^{\mathrm{k}} \quad . \quad . \quad . \quad . \quad . \quad . \quad . \quad . \quad . \quad (3)$$

The diffusion coefficients D_α^{k} in all phases α are regarded as constant, but could also easily be implemented as temperature dependent. The composition c_α^{k} of phase α is obtained from the partition coefficients $K_{\beta\alpha}$ between phase α and all other phases β and the phasefield parameter ϕ_β

$$c_\alpha^{\mathrm{k}} = \frac{c^{\mathrm{k}}}{\sum_{\beta=1}^{\mathrm{N}} \phi_\beta K_{\beta\alpha}^{\mathrm{k}}} \quad . \quad . \quad . \quad . \quad . \quad . \quad . \quad . \quad . \quad . \quad . \quad (4)$$

THERMODYNAMIC COUPLING

For IN706 alloy, a commercial nickel database from ThermoTech Ltd with 11 elements is used, from which the partition coefficients and the undercooling of the interfaces are calculated. Thermodynamic coupling is done using the TQ interface of Thermo-Calc software. Partition coefficients must be evaluated for all interface cells to obtain the phase compositions needed for the diffusion algorithm given by equation (4).

Growth kinetics of the shape function are determined using the average solutal undercooling $\Delta T_{\mathrm{solutal}}$ of the interface, calculated from the average composition by Thermo-Calc subroutines. Additionally, the curvature contribution $\Delta T_{\mathrm{curvature}}$ is calculated to obtain the kinetic undercooling of the interface ΔT

$$\Delta T = \Delta T_{\mathrm{solutal}} + \Delta T_{\mathrm{curvature}} \quad . \quad . \quad . \quad . \quad . \quad . \quad . \quad . \quad . \quad (5)$$

An exponential kinetic equation is used, comprising the sum of two terms for forward and backward motion of the solidification front

$$v = v_0 \left[\exp\left(\frac{\Delta T}{\Delta T_0}\right) - \exp\left(\frac{-\Delta T}{\Delta T_0}\right) \right] \quad . \quad . \quad . \quad . \quad . \quad (6)$$

Here v_0 and ΔT_0 are numerical parameters describing the mobility of the interface.

The undercooling in the region of the secondary arm is calculated separately to obtain the growth velocity in the [001] direction of the dendrite

$$v_{[001]} = v_0 \kappa \left[\exp\left(\frac{\Delta T_{[001]}}{\Delta T_0}\right) - \exp\left(\frac{-\Delta T_{[001]}}{\Delta T_0}\right) \right] \quad (7)$$

where κ is the kinetic anisotropy factor that increases the mobility in the [001] direction, assumed to have the value 1·05 in the present calculations. Using the two velocities v and $v_{[001]}$, L_0 and $L(0^\circ)$ in equation (1) can be obtained and the amplitude factor A can be calculated for each time step

$$A(t) = \frac{L(0^\circ,t)}{L_0(t)} - 1 \quad . \quad . \quad . \quad . \quad . \quad . \quad . \quad . \quad . \quad . \quad . \quad (8)$$

In this way $A(t)$ is included as an additional variable to allow the system to change continuously from cellular to dendritic, depending on the growth conditions, the diffusion coefficients, and the surface energy.

PRECIPITATION OF INTERDENDRITIC PHASES

The precipitation of secondary phases is an important factor in solidification processes, as it can be detrimental for the mechanical properties or can increase the homogenisation time necessary for their removal. In the present model secondary phases are included as circular shape functions, i.e. the amplitude factor A is restricted to zero. Nevertheless, after complete solidification the precipitates are not necessarily circular because they can be partially overgrown by the primary dendrites. Thus, the exact shape of the precipitates cannot be predicted from the model, but the volume fraction and the spatial distribution in the unit cell can. Interactions between solid phases are not included.

Nucleation is assumed to take place at the solid/liquid interface of the primary dendrite. For nucleation a certain undercooling ΔT_{nuc} is necessary. The local undercooling is calculated using Thermo-Calc and the thermodynamic database.

Results

TERNARY Ni–Al–Cr MODEL SYSTEM FOR NICKEL BASED SUPERALLOYS

Simulation was carried out using a ternary subsystem of the nickel data from ThermoTech, covering the elements Ni, Al, Co, Cr, Fe, Mo, Nb, Ti, Zr, B, and C. The diffusion

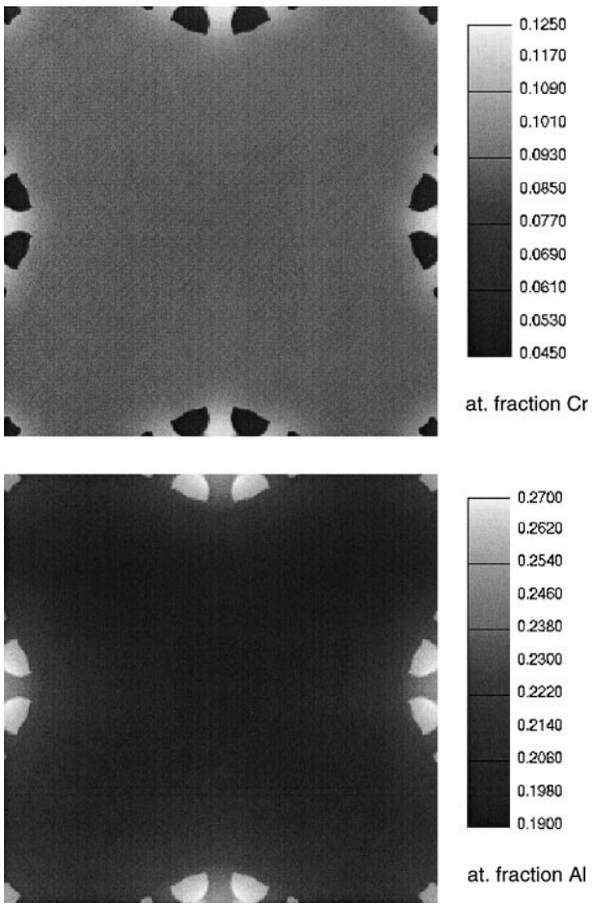

3 Composition distribution after complete solidification of ternary Ni–21Al–9Cr (at.-%) with interdendritic precipitation of γ'

coefficients in the γ phase were calculated from literature mobility data[15] to be $D_{Al}=2{\cdot}6\times10^{-12}$ m^2 s^{-1} and $D_{Cr}=7{\cdot}8\times10^{-13}$ m^2 s^{-1}. The same values were assumed for γ', while $D=1\times10^{-9}$ m^2 s^{-1} was taken for both components in the liquid. For precipitation of γ' the nucleation undercooling was estimated to be 1 K. The primary dendritic spacing λ_1 was assumed to be 250 μm.

Figure 3 shows the calculated microstructure and composition distribution of aluminium and chromium for a cooling rate of 0·5 K s^{-1}. It can clearly be seen that precipitation of the aluminium rich γ' particles takes place in the interdendritic region, while the γ dendrite shows a pronounced segregation pattern.

In Figure 4 the composition dependence of the γ' volume fraction is shown. It can be seen that a small variation in aluminium fraction has a strong influence on γ' precipitation.

IN706

For simulation of the commercial superalloy IN706 the nickel database from ThermoTech was reduced to the important elements, using composition (at.-%) Ni–18·5Cr–38·6Fe–1·81Nb–1·93Ti–(0–0·5)C. The diffusion coefficients for all elements were set to 1×10^{-9} m^2 s^{-1} in the liquid and 1×10^{-12} m^2 s^{-1} in all solid phases with the exception of carbon in fcc. For this place the diffusivity was chosen to be $D_C=1\times10^{-10}$ m^2 s^{-1}.

Nucleation was allowed for MC carbides, Laves phase, and η phase using a critical undercooling of 5 K for carbides and 2 K for the other phases. Under the applied conditions, only carbides and Laves phase occurred during simulation.

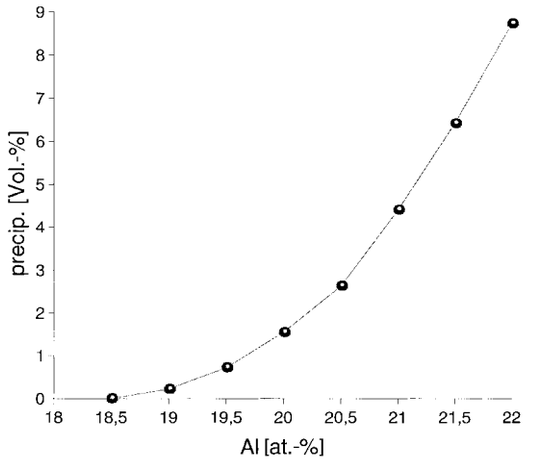

4 Variation of γ' volume with Al content in Ni–Al–Cr at constant Cr level of 9 at.-%

Figure 5 shows the calculated microstructure and composition distribution for chromium, niobium, and titanium under typical remelting conditions ($dT/dt=-0{\cdot}5$ K s^{-1}, $\lambda_1=200$ μm). Owing to their different chemical compositions, carbides and Laves phase which formed at the end of solidification in the remaining interdendritic melt can easily be distinguished from the primary dendrite.

In Fig. 6 the dependence of secondary phase precipitation on the carbon content is demonstrated. A higher carbon content not only increases the volume fraction of MC carbides, but at the same time reduces Laves formation because niobium and titanium are consumed by carbide precipitation. For comparison, the phase fractions from a straightforward Scheil type calculation are included as broken lines. As expected, the SCPF model predicts a lower Laves fraction owing to backdiffusion; but the amount of MC is raised significantly. This is because of carbon diffusion from the solid fcc dendrite to the carbides at the final solidification stage. It shows that in such complex multiphase systems results do not necessarily lie between the Scheil and the lever approximations.

Conclusion and outlook

In the presented model, sophisticated thermodynamic data are combined with 2D solidification simulation, taking into account solid and liquid diffusion and nucleation and growth of secondary phases. For this reason, valuable information can be expected to be obtained for commercial alloys such as nickel based superalloys.

One major problem encountered during modelling is the absence of literature data for several physical parameters which have a strong impact on the simulation results, such as diffusion coefficients, nucleation undercoolings, or surface energies and anisotropy. Some of these parameters, however, can be estimated by comparison with experiments.

For validation of the shape constrained phasefield (SCPF) model, experiments using different conditions and different alloys must be carried out. Of special importance for IN706 is the role of carbides, to be studied in the future using carbon enriched specimens. On this basis, more reasonable nucleation conditions in simulation should lead to a good agreement between the simulation and experiments.

Compared with the phasefield model, use of the fourfold shape function concept in the SCPF model allows a dramatic reduction of calculation effort. This is mainly a result of online coupling of thermodynamic data combined

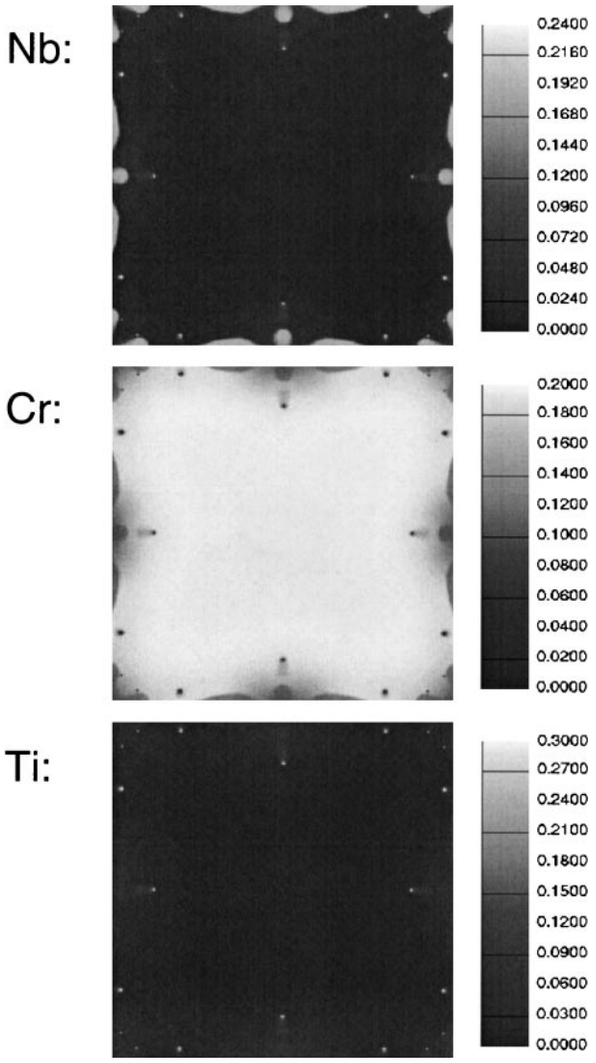

5 Composition distribution of Nb, Cr, and Ti (at. fraction) in IN706 calculated using shape constrained phasefield (SCPF) model

with the use of the shape function to obtain the driving force for the growing dendrite. However, as the shape function approach is held compatible with the phasefield algorithm, the latter could in the future be used just for secondary phases while the primary dendrite is further treated as a shape function. With this combination, homogenisation and solid phase transformations could be included, which would greatly enhance the capability of the model for microstructure prediction and alloy design.

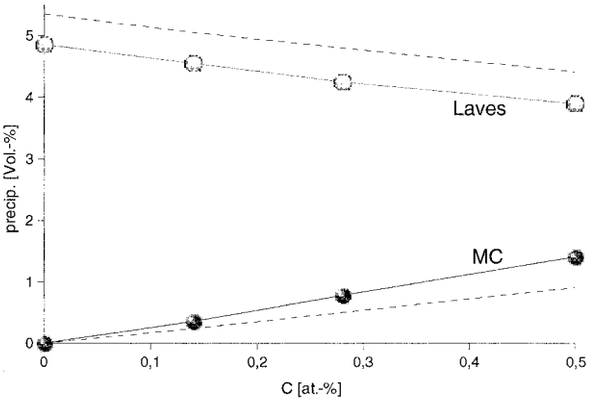

6 Variation of secondary phase volumes with C content in IN706 from SCPF model compared with Scheil approximation (dashed lines)

Acknowledgements

The authors wish to thank the DFG (Deutsche Forschungsgesellschaft) for financial support under grant number He200/4–1, and Dr Q. Chen and Professor B. Sundman for their assistance in use of the TQ interface.

References

1. T. HIMEMIYA and T. UMEDA: *ISIJ Int.*, 1998, **38**, 730–738.
2. D. MA and P. SAHM: *Metall. Trans. A*, 1992, **23A**, 3377–3381.
3. D. MA: *Giessereiforschung*, 1998, **50**, (1), 29–34.
4. T. KRAFT and H. E. EXNER: *Z. Metallkd.*, 1996, **87**, 652–660.
5. A. J. W. OGILVY and D. H. KIRKWOOD: *Appl. Sci. Res.*, 1987, **44**, 43–49.
6. A. ROÓSZ and H. E. EXNER: *Acta Metall. Mater.*, 1990, **38**, 2003–2016.
7. N. SAUNDERS and A. MIODOWNIK: 'CALPHAD, calculation of phase diagrams, a comprehensive guide' 1998, Oxford, Pergamon.
8. B. SUNDMAN, B. JANSSON, and J. O. ANDERSON: *Calphad*, 1985, **9**, 153–190.
9. N. SAUNDERS: in 'Superalloys 1996', (ed. R. D. Kissinger *et al.*), 101–110; 1996, Warrendale, PA, TMS.
10. D. A. KESSLER, J. KOPLIK, and H. LEVINE: *Phys. Rev. A*, 1986, **31**, 3352–3357.
11. J. D. HUNT: in 'Solidification and casting of metals', 3–9; 1979, London, The Metals Society.
12. D. GOLDSCHMIDT: *Materwiss. Werksttech.*, 1994, **25**, 311–320.
13. I. STEINBACH *et al.*: *Physica D*, 1996, **94**, 135–147.
14. J. TIADEN *et al.*: *Physica D*, 1997, **115**, 73–86.
15. A. ENGSTRÖM and J. ÅGREN: *Z. Metallk.*, 1996, **87**, 92–97.